

Tunable Reflectors Enabled Environment Augmentation for Better mmWave WLANs

Lan Zhang, Li Yan, Bin Lin, Yuguang Fang, and Xuming Fang

Abstract—With significant commercial potentials, millimeter-wave (mmWave) based wireless local area networks (WLANs) have attracted intensive attention lately. Unfortunately, the susceptible transmission characteristics over mmWave bands, especially the vulnerability to blockages, poses significant design challenges. Although existing solutions, such as beamforming, can overcome some of the problems, they usually focus on enhancing end transceivers to adapt to the transmission environments, and sometimes are still less effective. In this paper, by deploying highly-reflective cheap metallic plates as tunable reflectors without damaging the aesthetic nature of the environments, we propose to augment WLAN transmission environments in a way to create more effective alternative indirect line-of-sight (LOS) links by adjusting the orientations of the reflectors. Based on this idea, we design a novel adaptive mechanism, called *mmRef*, to effectively tune the angles of the deployed reflectors and develop corresponding operational procedures. Our performance study demonstrates our proposed scheme could achieve significant gain by tuning the angles of deployed reflectors in the augmented transmission environment.

Index Terms—Millimeter-Wave, Tunable Reflector, Transmission Environment Augmentation, WLAN.

I. INTRODUCTION

As the frontier of millimeter-wave (mmWave) commercial communication systems, wireless local area networks (WLANs) relying on IEEE 802.11ad or 802.11ay standard have attracted great attentions [2]–[5]. Although multi-gigabit data rate can be expected in mmWave WLANs, the poor characteristics of mmWave bands, especially the vulnerability of blockages, are urgently to be addressed. Due to the poor penetration and diffraction, as well as the nature of directional transmissions [2], an mmWave WLAN link can be easily blocked by obstacles, such as a furniture or a moving human body as shown in Fig.1, which cannot be solved by increasing the transmit power or directivity gain.

One intuitive solution is to utilize the more reliable sub-6GHz bands to compensate the blocked mmWave transmissions. However, the limited data rate through sub-6GHz bands (hundredfold data rate through mmWave bands) can hardly support mmWave WLAN applications, such as high-definition

multimedia and augmented reality [2]. Moreover, the integration will definitely burden the already crowded sub-6GHz bands. Recently, alternative links are considered in mmWave communications [6]–[8]. One way is to utilize mmWave relays to create multiple line-of-sight (LOS) paths. Although the relay technique is well-known in cellular systems, it is rarely utilized in WLANs due to the simplicity nature of the contention-based non-cooperative networking [3], [4]. Moreover, extra relays, especially with the expensive mmWave hardware, largely increase the cost of deploying the short-range WLANs. Even if a few mmWave relays can be afforded, due to the uncertainty of obstacles, LOS mmWave transmissions can still be hardly guaranteed.

Instead of using expensive mmWave relays, establishing alternative LOS links through reflections has recently aroused great attention [6]–[8]. Through bouncing off surrounding environments like wall and floor, Xue et al. proposed to concurrently transmit multiple reflected beams to one user [6]. However, the poor reflectance of surrounding environment like concrete and wood may lead to severe signal attenuation [9]. Fortunately, the cheap metallic plates with smooth surface can reflect nearly 100% signal strength. Using the metallic ceiling, Zhou, et al. enable several machine pairs simultaneously to communicate through mmWave bands in a data center, whose effectiveness is verified through the testbed [7]. Similar idea was used in multi-cubicle office for simultaneous mmWave transmissions [8]. However, unlike a data center used to store machines, WLANs are usually used by human beings, where the metal-coated ceiling will definitely lead to inconvenient and unattractive living environments. To address this issue, small-piece reflectors should be considered in mmWave WLANs. In addition, due to the strict reflection requirements (identical incidence and reflection angle), the angle of a reflector limits the direction of its reflected beam. Considering the mobility of user stations (STAs) as well as the unpredictability of blockages like the human body, reflectors with static angles may only serve STAs at certain positions. Thus, we propose to deploy tunable reflectors, small-piece metallic plates with adjustable angles, to augment mmWave WLAN transmission environments. To the best of our knowledge, none of existing research has considered this design.

In this paper, our fundamental idea is to deploy relatively cheap reflectors (comparing to other regular communication devices) without damaging the aesthetic nature of WLAN environments, and boost communication performance by tuning the angles of reflecting surfaces at the used reflectors. As a proof of concept, we first design a novel adaptive mechanism, called *mmRef* to implement tunable reflectors in mmWave

This work was partially supported by US National Science Foundation under grants CNS-1717736 and IIS-1722791.

Lan Zhang and Yuguang Fang are with Department of Electrical and Computer Engineering, University of Florida, Gainesville, FL, USA (email: lanzhang@ufl.edu, fang@ece.ufl.edu).

Li Yan and Xuming Fang are with Key Laboratory of Information Coding and Transmission, Southwest Jiaotong University, Chengdu 610031, China (email: liyan12047001@my.swjtu.edu.cn; xmfang@swjtu.edu.cn).

Bin Lin is with School of Information and Communications Engineering, Dalian Maritime University, Dalian, China (email: binlin@dlmu.edu.cn).

The extended version [1] has been under submission for journal publication.

WLANs. Specifically, we develop the system architecture from the concept of control-/data-plane decoupling [10], which integrates both the relatively reliable omni-directional low-frequency bands and the directional mmWave bands. Meanwhile, we design the operation procedures of *mmRef*, followed by the reflective link establishment scheme involving the signaling process and the smart reflector candidate selection algorithm (SRCS). To evaluate the expected performance benefits, we theoretically model the outage performance of our mechanism based on stochastic geometry theory. Simulation and numerical results finally demonstrate the effectiveness and the significant performance improvement of *mmRef* design.

The rest of this paper is organized as follows. Section II presents tunable reflector implementation design, and the reflective link establishment scheme is specifically presented in Section III. Section IV presents the analytical results of system performance modeling. Simulation and numerical results are evaluated in Section V. Section VI finally concludes this paper.

II. TUNABLE REFLECTOR IMPLEMENTATION DESIGN

To effectively implement tunable reflectors in mmWave WLANs, we propose a novel adaptive mechanism, *mmRef*. Specifically, we design the system architecture and operation procedures as follows.

A. The System Architecture

To mitigate the inherent blindness of directional mmWave transmissions while saving cost, the system architecture is developed from the concept of control-/data-plane decoupling [10]. As illustrated in Fig.1, the data-plane provides mmWave services with multi-gigabps data rate by mmWave access points (mmAP). The control-plan aims at coordinating the establishments of reflective links by selecting reflectors and tuning their angles, which is done by a controller. Physically, a controller could be a legacy AP using relatively reliable low-frequency bands with omni-directional coverage. Based on the control signaling, the angle of the reflector surface is adjusted to tune the reflected beam to serve surrounding STAs. Besides a smooth metallic plate, a reflector is equipped with a cost-effective low-frequency transceiver, such as the commercialized WLAN transceiver at 2.4GHz band. In addition, a simple mechanical device is equipped to rotate the metallic plate based on the control signaling. These tunable reflectors are deployed in the environment of interest, such as the ceiling of a room. To enable the reflective link between an mmAP-STA pair, the controller connects with mmAPs through either low-frequency links or deployed wired links, depending on specific applications. An STA is assumed to be equipped with both the low-frequency and mmWave transceivers for control-/data-plane signaling, respectively. When a transmission interruption occurs, the controller coordinates an mmAP and tunable reflectors to establish reflective links for an STA.

As a remark, we must point out that tuning the angles of reflectors in the transmission environment may take time and mechanical energy, and thus environment augmentation is usually used to reconfigure the overall networking environment in order to boost the overall network performance and should

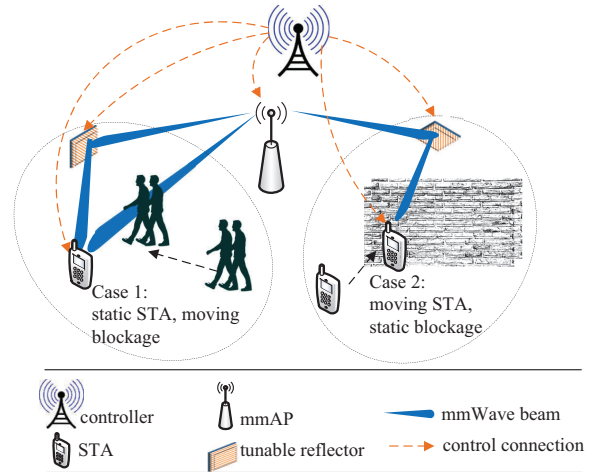


Fig. 1. The system architecture of *mmRef*.

be adaptively done at a larger time scale. Thus, adaptation must be done according to certain criterion, which is omitted in this paper.

B. Operation Procedures

To enable *mmRef* mechanism, we design the operation procedures among different system entities into two modules. The initialization module periodically acquires the information of serving entities, based on which the service module provides mmWave transmissions through reflective links.

1) As illustrated in Fig.2, the *Initialization Module* first generates the topology of all serving devices. Specifically, based on the location of mmAP n , the controller records the locations of all applicable reflectors for mmAP n in a table T_n , named as *MTable*. Instead of simply recording, T_n is a two-dimensional table with size $M \times J$, where each table element records information about a reflector, including its identity (ID), location, and usability (either idle or occupied). M and J represents the number of all beam directions of mmAP n and the maximal considered reflectors in one beam direction, respectively. Note that IEEE 802.11ad standard divides the 360° omnidirectional space into a set of equal-sized consecutive sectors $S = \{S_1, S_2, \dots, S_M\}$, where each sector corresponds to a beam direction with beam-width θ^{mmAP} , and $\theta^{mmAP} \times M = 360^\circ$. To adapt our reflective links to the directional transmissions based on IEEE 802.11ad standard, we record reflectors geographically located in different sectors in different rows, where reflectors in the i th row of T_n are located inside the i th sector of mmAP n . In addition, considering the severe distance-related propagation loss, with unknown STA locations and unpredictable blockages, a reflector geometrically closer to an mmAP is preferred due to the average better transmission performance brought by geometric proximity, which will be further discussed later. Thus, to better utilize deployed reflectors, the reflectors in a row of T_n are sorted in an ascending order based on their distances to mmAP n . As an example in Fig.2, reflector 1, 3 and 5 are located

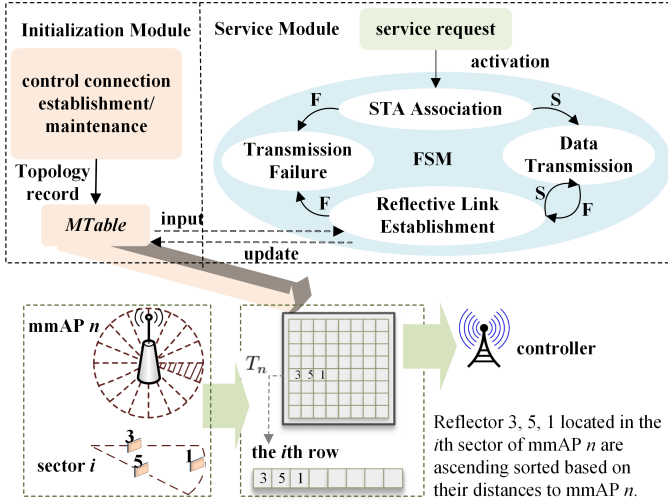


Fig. 2. The operation procedures of *mmRef*. Note state transition condition 'S' and 'F' respectively represent succeed and failed output.

inside sector i , and reflector 3 is the geometrically closest one to mmAP n .

2) The *Service Module* are operated based on a finite state machine (FSM), which is activated by the service request from an STA. In STA association state, an STA respectively connects to the controller and an mmAP, where the corresponding procedures of IEEE 802.11ad and 802.11g standard can be refereed [2]–[4]. In data transmission state, high-speed data transmissions are provided through the established direct or reflective links, either the links based on IEEE 802.11ad standard [2]–[4]. Both the transmission failure and data transmission states can terminate this FSM, and the corresponding feedback will be sent back to STAs. The reflective link establishment state is the core state of the FSM, aiming at selecting available reflectors and tuning to appropriate angles, which is detailed in next section.

III. REFLECTIVE LINK ESTABLISHMENT SCHEME

As the critical state in the service module, we present our reflective link establishment scheme. Specifically, we first design the signaling process, followed by the smart reflector candidates selection (SRCS) algorithm.

A. Signaling Process

As illustrated in Fig.3, the reflective link establishment process is initiated by an STA with an interrupted data transmission. The service request is sent to the controller in signaling 1), which carries the identity of the associated mmAP and the previous transmission sector S_i^n , based on which the controller checks the serving ability¹ of the mmAP in signaling 2). Once the service can be continuously provided, based on signaling 3), the controller sends back an acknowledgement (ACK) to the STA in signaling 4). Due to

¹The reason that serving ability of an mmAP is checked is to avoid the outage due to the inability of the mmAP to support the requested service.

Algorithm 1 Smart Reflector Candidate Selection (SRCS)

Input: mmAP n (T_n , S^n , N_S^n), STA i (S_i^n , $N_{i,RC}^n$).

Output: RC_i^n .

- // determining the selection sector area SS_i^n
- 1: Initialization: $m=i - \lfloor \frac{N_S^n}{4} \rfloor$, $\text{count}_{SS}=0$;
 - 2: **if** $N_{i,RC}^n < \lfloor \frac{N_S^n}{2} \rfloor$ **then**
 - 3: $\text{interv.SS} = \lfloor \frac{N_S^n}{2} \rfloor / N_{i,RC}^n$, $SS_i^n = \emptyset$;
 - 4: **while** $\text{count}_{SS} < N_{i,RC}^n$ **do**
 - 5: $SS_i^n = \{SS_i^n, S_m^n\}$, $m=m+\text{interv.SS}$, $\text{count}_{SS}++$;
 - 6: **end while**
 - 7: **else**
 - 8: $\text{multi.SS} = \lfloor \frac{N_S^n}{2} \rfloor / N_{i,RC}^n$;
 - 9: $SS_i^n = \bigcup_{\text{multi.SS}} \{S_{i \pm m}^n | m \in [0, \lfloor \frac{N_S^n}{2} \rfloor]\}$;
 - 10: **while** $\text{count}_{SS} < N_{i,RC}^n - \text{multi.SS} \cdot \lfloor \frac{N_S^n}{2} \rfloor$ **do**
 - 11: $SS_i^n = \{SS_i^n, S_m^n\}$, $m=m+\text{interval.SS}$, $\text{count}_{SS}++$;
 - 12: **end while**
 - 13: **end if**
- // determining reflector candidates RC_i^n inside SS_i^n
- 14: Initialization: $\text{count}_{RC}=0$, $RC_i^n = \emptyset$;
 - 15: **while** $\text{count}_{RC} < N_{i,RC}^n$ **do**
 - 16: Find the first element in the row corresponding to sector SS_i^n (count_{RC}) with idle state, and mark it as occupied;
 - 17: $\text{count}_{RC}++$;
 - 18: **end while**

the unknown locations of the STA and blockages, we design Algorithm 1 (smart reflector candidate selection, SRCS) to effectively select available reflectors, which will be detailed later. The controller informs the reflector angle tuning (RAT) process to the selected reflector candidates in signaling 5). Once ACKs are sent back from the reflectors in signaling 6), the controller assigns them to the mmAP in signaling 7) and receives an ACK in signaling 8). After the synchronization in signaling 9), the controller coordinates the mmAP, STA and reflectors for simultaneous RAT. Based on the feedback from the STA, the controller respectively informs the mmAP, STA and the selected reflectors in signaling 10). Once the ACKs are received in signaling 11)–13), the approved reflective link is sent in signaling 14) and the data transmission through a reflective link can start.

B. SRCS Algorithm

Due to the tunable design, all reflectors surrounding an mmAP can be reflector candidates for reflector angle tuning (RAT) to further discover the final serving reflective links. For the reflector candidate selection, there are several challenges: 1) The number of reflector candidates should be limited to reduce the cost and overhead introduced by more reflected beams. 2) The channel state information (CSI) of a reflective link, i.e., the usability of a reflector, cannot be known before training its angle. 3) The controller does not know exact locations of dynamic STAs and blockages, which can only be inferred from the previous interrupted transmissions.

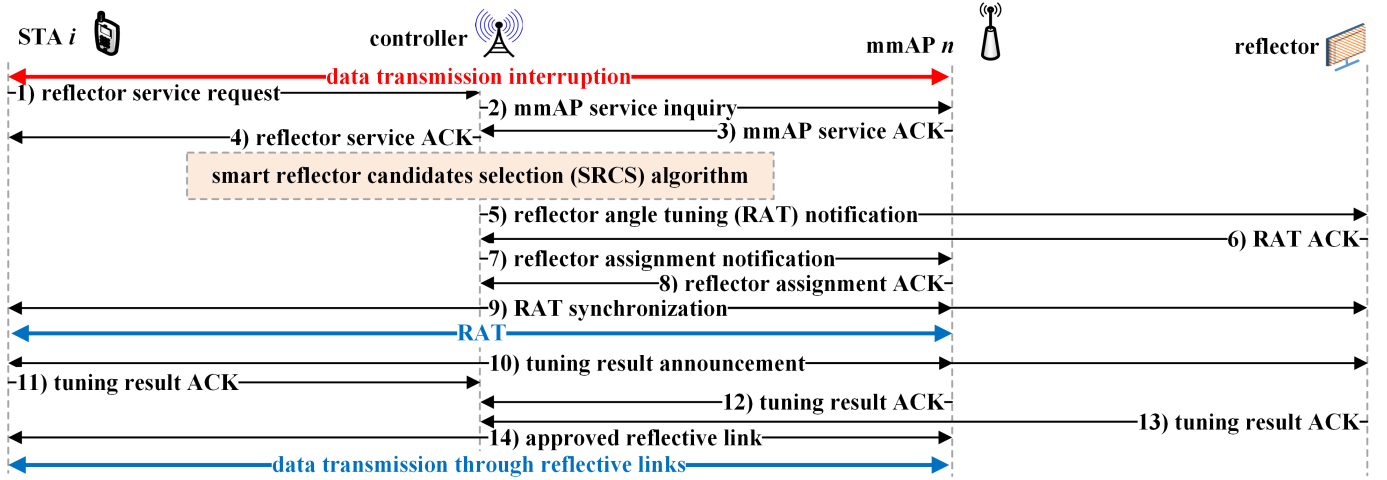


Fig. 3. The signaling process of reflective link establishment. The black and blue lines respectively represent the control and data transmissions.

To address these challenges, a heuristic algorithm, smart reflector candidate selection (SRCS), is proposed to effectively work on a small group of reflectors with relatively good performance. For an interrupted transmission, we can infer that the locations of the STA and blockages are inside or close to the previous transmission sector. Denote the previous transmission sector of mmAP n towards STA i by S_i^n , which can be acquired based on IEEE 802.11ad standard [2]. According to the $MTable$ illustrated in Fig.2, reflectors in T_n are ordered by their geometric locations of mmAP sectors. Since blockages are usually unpredictable, reflector candidates denoted by RC_i^n should be scattered over the environment to increase link diversity. Thus, we first determine the area of RC_i^n selection in the form of mmAP sectors, and then find the specific RC_i^n located inside these sectors. Denote the size of RC_i^n by $N_{i,RC}^n$, which is assigned by the controller. Since a reflector is only located inside one mmAP sector, denote the sector set of RC_i^n by SS_i^n , where $|SS_i^n| = N_{i,RC}^n$. Instead of selecting specific reflectors for RC_i^n , the corresponding sector area is first selected to guarantee the diversity of reflective links. Since the reflectors around the mmAP n and STA i pair are preferred, we only consider a half of sectors $\{S_{i\pm m}^n | m \in [0, \lceil N_S^n/4 \rceil]\}$ towards STA i as the pool of SS_i^n selection area, where N_S^n is the sector number of mmAP n . Note that the same sector may exhibit more than once in SS_i^n when the required reflector candidates are more than the considered sectors, i.e., $N_{i,RC}^n > \lceil N_S^n/2 \rceil$. The basic idea of SS_i^n selection is their diversely scattered locations (Algorithm 1 line 1-13). When the number of assigned reflector candidates is few (say, $N_{i,RC}^n < \lceil N_S^n/2 \rceil$), the selected sectors of SS_i^n should try to be disconnected. Otherwise, the RC_i^n should be evenly distributed in the sector pool. Based on the determined SS_i^n , we select specific reflectors as RC_i^n inside each sector of SS_i^n . Since a longer transmission distance introduces larger attenuation and more probable blockages, we take the proximity benefits into account. Considering the unknown accurate location of STA i , the reflector closer to mmAP n is selected with priority, which are the first idle

reflector in the row (sector) belonging to SS_i^n in $MTable T_n$. To avoid duplicated assignment, the selected reflector should update its availability state as occupied.

By using the selected reflector candidates, the controller coordinates their angle tuning simultaneously until applicable reflective links are searched. The detailed SRCS algorithm are summarized in Algorithm 1.

IV. THEORETICAL SYSTEM PERFORMANCE MODELING

As a proof of concept, we then theoretically quantify the benefits of implementing the aforementioned *mmRef*. Based on stochastic geometry theory, we model the outage performance in mmWave WLANs. Besides our *mmRef* mechanism, two cases involving reflective transmissions are considered for comparison. Specifically, in one case, we consider deploying static metallic plates, where the applicable reflectors, satisfying equal incidence and reflection angles for an mmAP-STA pair, may be largely reduced or even non-existing. In the other case, environmental reflectors are used, such as wood or concrete with poor reflectance, where the reflective links are established through sweeping the environment. For simplicity, we respectively define the *mmRef*, static reflector deployment and environmental reflector cases as Case 1-3.

Due to the page limit, this paper ignores the assumptions, system setting, modeling and proof, and only presents the analytical results of the outage probabilities respectively in the three cases, which are numerically evaluated in the evaluation section. The detail can be found in [1].

Theorem 1. The outage probability of the mmWave transmission through a reflective link in Case $i \in \{1, 2, 3\}$ can be given by

$$Pr_{\text{ref}}^i \triangleq \sum_{n=0}^{N_h} \binom{N_h}{n} (-1)^n \left\{ G_i + \int_{D_0}^{\infty} \Pr(D > d) g'_i(d) dd \right\}, \quad (1)$$

where N_h is the channel parameter, D_0 is the distance between the STA and mmAP, and $Pr(D > d)$ is the cumulative proba-

TABLE I
PARAMETERS OF PERFORMANCE EVALUATION

Parameter	Value	Description
D_0	10 m	direct link distance
α_L, α_N	2, 4	pathloss exponent (LOS, NLOS)
N_{hi}	3	Nakagami fading parameter
β	0.008	parameter of blockage model
λ_1	$0.01/m^2$	intensity of reflectors in <i>mmRef</i>
$\gamma_1, \gamma_2, \gamma_3$	1, 1, 0.5	reflector reflectance (case 1, 2, 3)
P_s/σ^2	5×10^5	transmit power to noise power ratio
ϵ	0 dB	SNR threshold

bility distribution (CDF) of the shortest reflective link distance of the mmAP-STA pair. The expression of $Pr(D > d)$, G_i , b_i , and g'_i , and the proof are detailed in [1].

According to the design of *mmRef* mechanism in Section III and IV, a reflective link is established when a transmission interruption occurs. Once the direct transmission is blocked, the transmission can be recovered by a reflective link. Thus, outage probability of the mmWave WLANs assisted by a reflective link provided by *mmRef* mechanism is given by $Pr^i = Pr_{O,d} \cdot Pr_{O,r}^i$, where Case $i \in \{1, 2, 3\}$, and $Pr_{O,d}$ is the outage probability of direct link transmission with distance D_0 derived based on (1) with $\gamma_i = 1$ and $D = D_0$.

V. PERFORMANCE EVALUATION

As a proof of concept, this work focuses on how to implement *mmRef* and what performance benefits can be expected from the established reflective links. Based on analysis from the previous two sections, simulation and numerical results are presented below. Unless specified otherwise, the system parameters in Table I will be used [11]–[14].

To verify the **effectiveness of implementing *mmRef*** to establish reflective links, we first evaluate the performance of SRCS. Fig.4 illustrates the performance of the SRCS algorithm, where the frequency of the LOS transmissions, i.e., the possibility of successfully recovered transmissions, is as a function of different blocking conditions in terms of different locations and sizes of blockages. Since the SRCS algorithm is designed to intelligently select reflector candidates to circumvent the unknown blockages, we examine the recovery results based on the SRCS algorithm. Due to the aforementioned challenges in our reflector candidate selection, we utilize random selection as the baseline. We observe that the successful recovery probability is significantly improved by utilizing the SRCS algorithm compared with that by using random selection. In most blocking conditions, the successful recovery can be perfectly guaranteed by the SRCS algorithm. Even in some extreme conditions where the blockages are very close to the STA or mmAP, the recovery results are also attractive.

Based on the theoretical modeling, we then evaluate the outage performance to examine the **performance benefits expected from *mmRef***. For a fair comparison, the three Cases in Section IV are evaluated under the same system setting. The reflector intensity of Case 1 is $\lambda_1 = 0.01/km^2$ and the reflectance in case 1 and 2 is $\gamma_1 = \gamma_2 = 1$. To validate the accuracy of our analytical results, Monte Carlo simulation

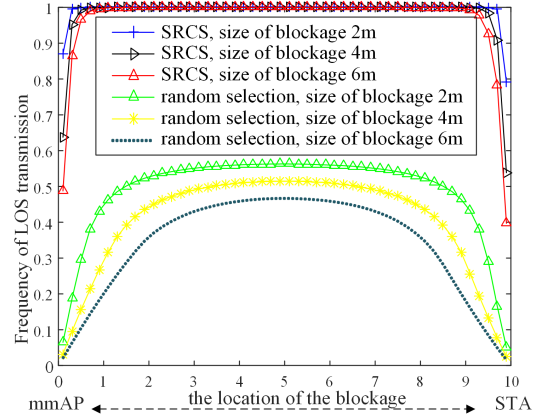
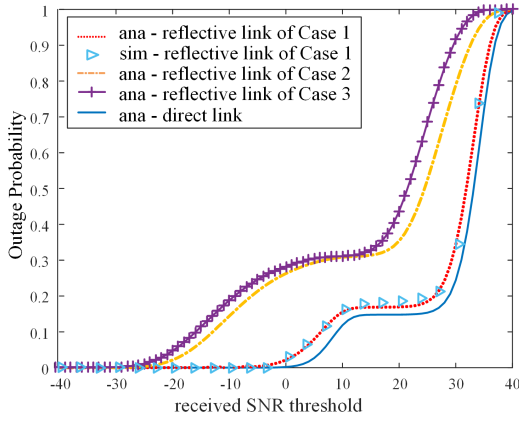


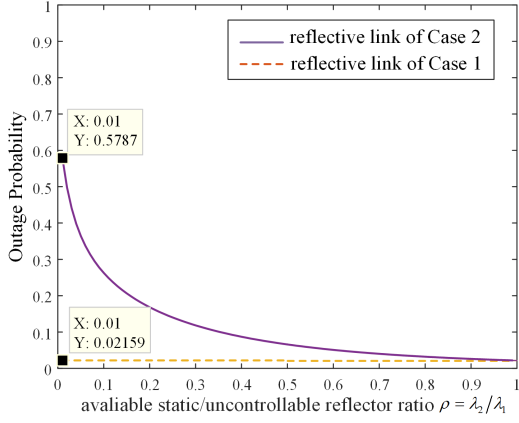
Fig. 4. Performance of reflective-link establishment scheme.

results are provided with the same parameters through 10,000 independent realizations in a square area of $500m \times 500m$.

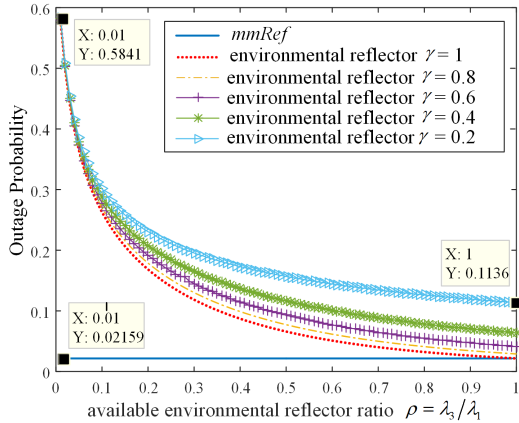
Fig.5 illustrates the outage performance comparison among the three cases. The overall performance of the three cases are evaluated in Fig.5(a), where the outage probability is as a function of the received SNR threshold, where $\lambda_2 = \lambda_3 = 0.001/m^2$ and $\gamma_3 = 0.5$. We observe that the outage probability of Case 1 is much lower than that of Case 2 and 3, which validates the effectiveness of the reflective link provided by *mmRef*. In addition, the outage probability of Case 1 is close to that of the direct link, which reveals that although outages may occur more frequently in reflective links due to the longer distances compared with the direct link, the performance of *mmRef* is very close to the best. Comparison between Case 1 and 2 is illustrated in Fig.5(b), where the outage probability is as a function of the ratio of available reflectors to the deployed reflectors. Although the static reflectors in Case 2 lower the cost of system deployment, their services are restricted to certain areas. Given the same number of deployed reflectors in Case 1 and 2, the available reflectors in Case 2 is much fewer with intensity $\lambda_2 = \rho_{1,2}\lambda_1$. We observe that when $\rho_{1,2} = 0.01$, the outage probability of case 2 is nearly 30 times compared with that of Case 1, which reveals that the static reflectors can achieve a comparable performance only when a massive number of them are deployed. Case 1 and 3 are evaluated in Fig.5(c), where the outage probability is as a function of the ratio of available environmental reflectors to the deployed tunable reflectors. Different from Case 2, the environmental reflectors may largely attenuate the signal strength with low reflectance γ_3 . We observe that the outage becomes very severe when γ_3 becomes small. Even with enough environmental reflectors, i.e., $\rho_{1,3} = 1$, the outage probability of Case 3 is still 5 times higher than that of Case 1. Moreover, the poor reflection characteristics due to the property of different materials, such as wood and concrete [9], cannot be overcome. Therefore, compared with Case 2 and 3, robust mmWave transmissions through reflective links can be expected by implementing *mmRef*. Simulation results further validate the accuracy of our modeling. Although the outage probability of the analytical results are a little lower than that



(a) Overall comparison.



(b) Comparison between Case 1 and 2.



(c) Comparison between Case 1 and 3.

Fig. 5. The outage performance comparisons for the three cases through the reflective link.

in the simulation results, the analytical results can be a lower bound effectively characterizing the system performance.

VI. CONCLUSION

In this paper, we have investigated how to augment the transmission environments of mmWave WLANs to boost the network performance, while not damaging the aesthetic nature of the environment, by deploying tunable reflectors, the highly-reflective cheap metallic plates with adjustable

angles. To realize this idea, we have designed a novel adaptive mechanism, called *mmRef*, to effectively tune the angles of the deployed reflectors when necessary. Specifically, we have developed the system architecture from the idea of decoupling control-/data-signaling. Based on the centralized control, the operation procedures and the reflective link establishment scheme with the signaling processing and algorithm design can be effectively implemented. We have also conducted theoretical study on the performance based on stochastic geometry theory. Our simulation and numerical results have demonstrated the effectiveness of implementing *mmRef* and the significant performance gain from our design. We expect our preliminary study will inspire more thorough research on this approach.

REFERENCES

- [1] L. Zhang, L. Yan, B. Lin, H. Ding, Y. Fang, and X. Fang, "Augmenting transmission environments for better communications: tunable reflector assisted mmwave w lans," <http://www.fang.ece.ufl.edu/drafts/augmenting4journal.pdf>, to be submitted for journal submission.
- [2] A. Ghosh, T. A. Thomas, M. C. Cudak, R. Ratasuk, P. Moorut, F. W. Vook, T. S. Rappaport, G. R. MacCartney, S. Sun, and S. Nie, "Millimeter-wave enhanced local area systems: A high-data-rate approach for future wireless networks," *IEEE Journal on Selected Areas in Communications*, vol. 32, no. 6, pp. 1152–1163, 2014.
- [3] W. G. Alliance, "Wigig white paper: Defining the future of multi-gigabit wireless communications," <http://wirelessgigalliance.org/specifications/>, 2010.
- [4] T. Nitsche, C. Cordeiro, A. B. Flores, E. W. Knightly, E. Perahia, and J. Widmer, "Ieee 802.11 ad: directional 60 ghz communication for multi-gigabit-per-second wi-fi," *IEEE Communications Magazine*, vol. 52, no. 12, pp. 132–141, 2014.
- [5] P. Zhou, K. Cheng, X. Han, X. Fang, Y. Fang, R. He, Y. Long, and Y. Liu, "Ieee 802.11 ay-based mmwave w lans: Design challenges and solutions," *IEEE Communications Surveys & Tutorials*, vol. 20, no. 3, pp. 1654–1681, 2018.
- [6] Q. Xue, X. Fang, and C.-X. Wang, "Beamspace su-mimo for future millimeter wave wireless communications," *IEEE Journal on Selected Areas in Communications*, vol. 35, no. 7, pp. 1564–1575, 2017.
- [7] X. Zhou, Z. Zhang, Y. Zhu, Y. Li, S. Kumar, A. Vahdat, B. Y. Zhao, and H. Zheng, "Mirror mirror on the ceiling: Flexible wireless links for data centers," *ACM SIGCOMM Computer Communication Review*, vol. 42, no. 4, pp. 443–454, 2012.
- [8] Z. Shi, R. Lu, J. Chen, and X. S. Shen, "Three-dimensional spatial multiplexing for directional millimeter-wave communications in multicube office environments," in *2013 IEEE Global Communications Conference (GLOBECOM)*. IEEE, 2013, pp. 4384–4389.
- [9] B.-G. Choi, W.-H. Jeong, and K.-S. Kim, "Characteristics analysis of reflection and transmission according to building materials in the millimeter wave band," *power (dBm)*, vol. 13, no. 50.62, pp. 64–48, 2015.
- [10] L. Yan, X. Fang, and Y. Fang, "Control and data signaling decoupled architecture for railway wireless networks," *IEEE Wireless Communications*, vol. 22, no. 1, pp. 103–111, 2015.
- [11] T. Bai, R. Vaze, and R. W. Heath, "Analysis of blockage effects on urban cellular networks," *IEEE Transactions on Wireless Communications*, vol. 13, no. 9, pp. 5070–5083, 2014.
- [12] J. G. Andrews, T. Bai, M. N. Kulkarni, A. Alkhateeb, A. K. Gupta, and R. W. Heath, "Modeling and analyzing millimeter wave cellular systems," *IEEE Transactions on Communications*, vol. 65, no. 1, pp. 403–430, 2017.
- [13] K. Venugopal, M. C. Valenti, and R. W. Heath, "Device-to-device millimeter wave communications: Interference, coverage, rate, and finite topologies," *IEEE Transactions on Wireless Communications*, vol. 15, no. 9, pp. 6175–6188, 2016.
- [14] A. Thornburg, T. Bai, and R. W. Heath Jr, "Performance analysis of outdoor mmwave ad hoc networks," *IEEE Trans. Signal Processing*, vol. 64, no. 15, pp. 4065–4079, 2016.